the wake-integral theory since, when implemented computationally, the force integrals in Eqs. (4) and (9) involve summation over the entire S_2 plane. In theory the only contributions to these integrals should come from the vorticity present in the infinitesimally thin vortical sheet shed behind the wing. However, because of numerical dissipation, this sheet obtains a finite thickness forming a vortical wake, making it difficult if not impossible to isolate it from the surrounding low-level vortical field. Though the background vorticity level is several orders in magnitude smaller than that present in the vortical sheet (wake), it is spread over an area several orders larger than that constituting the vortical sheet. Consequently, when this low-level background vorticity is included, the errors in the force integrals were observed to be significant. This dilemma is somewhat analogous to determining the edge of a boundary layer, which is arbitrarily defined. It cannot be overemphasized how critical a role the definition of the vortical wake edge plays in determining the prediction performance of this wake-integral method.

The approach adopted to circumvent this problem was to employ a vorticity filter. This filter was constructed by setting a threshold value for vorticity, and any vorticity values smaller than this threshold were then dropped out. The correct filter was obtained iteratively by selecting a threshold value and computing the lift coefficient using the wake-integral method. Since the lift coefficient using surface pressure integration is a proven good estimate of the true lifting characteristics of a body, the lift coefficient obtained from wake integration was compared with that obtained from surface pressures. The filter level that yielded a match (within a given tolerance) was selected as the correct filter for that case. The stream function and the drag integral were then computed using that filter. Since finding the edge of the vortical wake was found to be a function of the particular problem being simulated, a new filter threshold value had to be set for each case.

The results presented in the table indicate that the wake-integral method is accurate in predicting the lift-induced drag for a finite wing. It should be noted, however, that an accurate resolution of the vortical sheet is absolutely indispensable in this approach, since the more the vorticity in the sheet is dissipated (again forming what amounts to a wake), the greater the ambiguity in determining its extent into the surrounding field.

Conclusions

The capacity to predict drag due to lift using numerical simulations of the flowfield and a wake-integral approach has been studied. An important finding during the course of this research was the presence of low-level spurious vorticity in the flow. Future work must address the problem of requiring arbitrary filters to determine the extent of the vortical wake that ultimately governs the integral limits. Since the postprocessor uses a wake-based approach to compute the lift and drag about a lifting body, it was found that to correctly predict these force components it is necessary to very accurately resolve the flowfield in this region. An accurate resolution of the vortical field is critical when using the present approach for induced drag calculations. To maintain the performance of this approach, a sufficiently dense mesh is required in the wake region. This yields somewhat of a tradeoff situation since the errors associated with surface pressure integration can also be reduced with a sufficient increase in mesh density local to the body. Perhaps the use of a computational method specifically designed for the unmolested transport of vorticity would be the ultimate complement to the wake-integral method.

Acknowledgments

Funding for this project was provided by NASA Grant NAG-1-1271, with Dennis Bartlett as technical monitor. The authors would also like to thank the Mississippi Center for Supercomputing Research for providing several hours of Cray time for project software debugging and a portion of the runs presented here.

References

[1]Henderson, W. P., and Holmes, B. J., "Induced Drag—Historical Perspective," Society of Automotive Engineers, SAE Technical Paper Series, SAE Aerotech 1989 Conf., Sept. 1989.

[2]Janus, J. M., Chatterjee, A., and Cave, C., "Computational Analysis of Methods for Reduction of Induced Drag," AIAA Paper 93-0524, Jan. 1993.

[3]Wu, J. C., Hackett, J. E., and Lilley, D. E., "A Generalized Wake-Integral Approach for Drag Determination in Three-Dimensional Flows," AIAA Paper 79-0279, Jan. 1979.

[4]van Dam, C. P., Nikfetrat, K., Vijgen, P. M. H. W., and Fremaux, C. M., "Calculation and Measurement of Induced Drag at Low Speeds," Society of Automotive Engineers, SAE Paper 901935, Oct. 1990.

[5]van Dam, C. P., Chang, I. C., Vijgen, P. M. H. W., and Nikfetrat, K, "Drag Calculations of Wings Using Euler Methods," AIAA Paper 91-0338, Jan. 1991.

[6]Chatterjee, A., "Numerical Prediction of Induced Drag for Wings and Wing–Body Combinations," M.S. Thesis, Dept. of Aerospace Engineering, Mississippi State Univ., Mississippi State, MS, Dec. 1993.

[7]Lamb, H., *Hydrodynamics*, 6th ed., Dover, New York, pp. 219, 220.

New Mixed Van Leer Flux Splitting for Transonic Viscous Flow

Pascal Ferrand* and Stéphane Aubert†
École Centrale de Lyon, Ecully 69131, France

Introduction

THE Van Leer[1] (VL) scheme is a very popular flux vector splitting method used for inviscid transonic flow. It presents an excellent shock capturing capability with few oscillations in these areas. It has been demonstrated that the VL method has the ability and robustness to capture intense nonlinear waves, but it is well known that it generates an excess of diffusion at low Mach number. Indeed, this method is efficient for Euler equations discretization in transonic applications but not for Navier–Stokes equations discretization. On the other hand, the central schemes (CS) give very good accuracy in the boundary layer, but may allow large oscillations and losses across shocks. Different alternatives have been developed. For example, flux difference splitting[2] presents better accuracy through the contact discontinuities. Another way consists of modifying the original VL scheme to minimize the numerical error, with more[3,4] or less[5] success. Various hybridizing schemes have been also developed by several authors; see, for example, Coquel and Liou.[6] Basically, these approaches combine two complementary schemes by choosing the best scheme for each point of the grid.[4]

In this Note, we propose an alternative to the hybrid scheme that is very simple and resolves the same difficulties at the interface of the different schemes. Additionally, the introduction of this formulation is quasi-immediate in all VL MUSCL methods. This new approach is based on VL flux vector splitting and called the mixed VL method (MVL). The proposed MVL method has been constructed to conserve the advantages of the CS method at low Mach number and the advantages of the VL method elsewhere. This construction is based on the same VL principles to define the fluxes, and keeps the monoticity condition by defining an adapted weighting function between the CS and the VL scheme.

New MVL Method

In this Note, our objectives are the following: 1) to obtain an efficient modification at low Mach number, 2) to conserve the VL properties through the shocks, 3) to define a formulation easy to incorporate in existing VL methods, 4) to eliminate supplementary tests of local flow conditions, and 5) to limit the increase of memory and CPU time.

Received May 11, 1994; revision received July 21, 1995; accepted for publication July 25, 1995.

*Research Scientist, Laboratoire de Mécanique des fluides et d'acoustique, Centre National de la Recherche Scientifique, URA 263, Université Lyon I.

†Associate Professor, Laboratoire de Mécanique des fluides et d'acoustique, Éducation Nationale, Université Lyon I.

Our technique can be very easily incorporated into all of the VL flux splitting methods. To illustrate this, we incorporate it into a finite volume formulation here.

The MVL method has been introduced in a code PROUST that was designed to compute three-dimensional viscous flows in turbomachinery where the interactions of waves and coupling between flow and structure occur. It is based on a finite volume formulation over structured quadrangular meshes. The time discretization uses an explicit second-order Runge–Kutta schemes with five steps. The diffusive fluxes are computed using a second-order central difference scheme. Compatibility relations are introduced to treat all boundary conditions. The method is completely described by Aubert et al.[7] We just present here the principle of introduction of the MVL method.

The three-dimensional compressible Navier–Stokes equations in curvilinear space are

$$\frac{\partial \boldsymbol{q}}{\partial \tau}+\frac{\partial \boldsymbol{E}}{\partial \xi}+\frac{\partial \boldsymbol{F}}{\partial \eta}+\frac{\partial \boldsymbol{G}}{\partial \gamma}=\frac{1}{Re}\left(\frac{\partial \boldsymbol{E}_v}{\partial \xi}+\frac{\partial \boldsymbol{F}_v}{\partial \eta}+\frac{\partial \boldsymbol{G}_v}{\partial \gamma}\right)$$

where $\boldsymbol{E}, \boldsymbol{F}$, and $\boldsymbol{G}$ are the convective fluxes, $\boldsymbol{E}_v, \boldsymbol{F}_v$, and $\boldsymbol{G}_v$ are the diffusive fluxes, Re is the Reynolds number, $\boldsymbol{q}$ is the three-dimensional state vector $\{\rho, \rho u, \rho v, \rho w, \rho e_0\}$ or $\{q_1, q_2, q_3, q_4, q_5\}$. Also (u, v, w) are the velocity components in the ξ, η, γ directions, τ is the time, and ρ and e_0 are the density and the total energy, respectively.

A MUSCL approach is used to evaluate the flux; the conservative variables q (the variable indice is omitted for clarity) are interpolated on cell surfaces, then the flux is evaluated. Finally, the gradient can be discretized as

$$E_{i+\frac{1}{2}}-E_{i-\frac{1}{2}}=E^{+}\left(q^{-}_{i+\frac{1}{2}}\right)-E^{+}\left(q^{-}_{i-\frac{1}{2}}\right)+E^{-}\left(q^{+}_{i+\frac{1}{2}}\right)-E^{-}\left(q^{+}_{i-\frac{1}{2}}\right)$$

with $q^{+}_{i+1/2}$ and $q^{-}_{i+1/2}$ the down- and upwind variables, respectively.

In this case, the VL flux can be written at point $i-\frac{1}{2}$ as

$$E_{\mathrm{VL}_{i-\frac{1}{2}}}=E^{+}\left(q^{-}_{i+\frac{1}{2}}\right)+E^{-}\left(q^{+}_{i+\frac{1}{2}}\right)$$

with the conservative variables $q^{\pm}$ defined by

$$q^{+}_{\mathrm{VL}_{i-\frac{1}{2}}}=\tfrac{1}{4}\phi(\kappa\phi-1)q_{i+1}+\left(1-\tfrac{1}{2}\kappa\phi^{2}\right)q_i+\tfrac{1}{4}\phi(1+\kappa\phi)q_{i-1}$$

$$q^{-}_{\mathrm{VL}_{i-\frac{1}{2}}}=\tfrac{1}{4}\phi(1+\kappa\phi)q_i+\left(1-\tfrac{1}{2}\kappa\phi^{2}\right)q_{i-1}+\tfrac{1}{4}\phi(\kappa\phi-1)q_{i-2}$$

where the limiter ϕ and the parameter κ determine the precision between the first and the third order. In the particular case where ϕ and κ are equal to one, the variables q^{+}_{VL} and q^{-}_{VL} are identical,

$$q^{+}_{\mathrm{VL}_{i-\frac{1}{2}}}=q^{-}_{\mathrm{VL}_{i-\frac{1}{2}}}=qc_{i-\frac{1}{2}}=\tfrac{1}{2}(q_i+q_{i-1})$$

and the VL flux E_{VL} is equal to the full flux E_C

$$E_{\mathrm{VL}}=E^{+}_{\mathrm{VL}}+E^{-}_{\mathrm{VL}}=\tfrac{1}{2}E_C+\tfrac{1}{2}E_C=E_C$$

We obtain a second-order central scheme. Therefore, following the local Mach number, we define a new MVL flux composed of both a full flux and a VL flux. Thus, we can write the new flux E_{MVL} as a function of the VL flux E_{VL}, the complete flux E_C, and a MVL function Ψ_{MVL} in term of conservative variables,

$$q^{\pm}_{\mathrm{MVL}_{i-\frac{1}{2}}}=\Psi_{\mathrm{MVL}}q^{\pm}_{\mathrm{VL}_{i-\frac{1}{2}}}+(1-\Psi_{\mathrm{MVL}})qc_{i-\frac{1}{2}}$$

or in term of fluxes,

$$E^{+}_{\mathrm{MVL}}=\Psi_{\mathrm{MVL}}E^{+}_{\mathrm{VL}}+\frac{(1-\Psi_{\mathrm{MVL}})}{2}E_C$$

$$E^{-}_{\mathrm{MVL}}=\Psi_{\mathrm{MVL}}E^{-}_{\mathrm{VL}}+\frac{(1-\Psi_{\mathrm{MVL}})}{2}E_C$$

The weighting function Ψ_{MVL} is generated to satisfy the continuity of the scheme and to reduce the influence of VL numerical viscosity. Therefore, Ψ_{MVL} is a function of the Mach number and equal to zero when the Mach number is zero, and it is equal to one at an arbitrary linking Mach number M_l. Thus, the MVL flux respects the following conditions.

When $M=0$:

$$E^{+}_{\mathrm{MVL}}=\tfrac{1}{2}E_C \qquad E^{-}_{\mathrm{MVL}}=\tfrac{1}{2}E_C$$

When $M=M_l$:

$$E^{+}_{\mathrm{MVL}}=E^{+}_{\mathrm{VL}} \qquad E^{-}_{\mathrm{MVL}}=E^{-}_{\mathrm{VL}}$$

Different choices of the function Ψ_{MVL} are possible, but to preserve the features of the VL flux, this function must be built with the same continuity principles as those of the VL flux. The supplementary conditions are as follows.

When $M=0$:

$$\frac{\partial\left(E^{+}_{\mathrm{MVL}}+E^{-}_{\mathrm{MVL}}\right)}{\partial M}=\frac{\partial E_C}{\partial M}$$

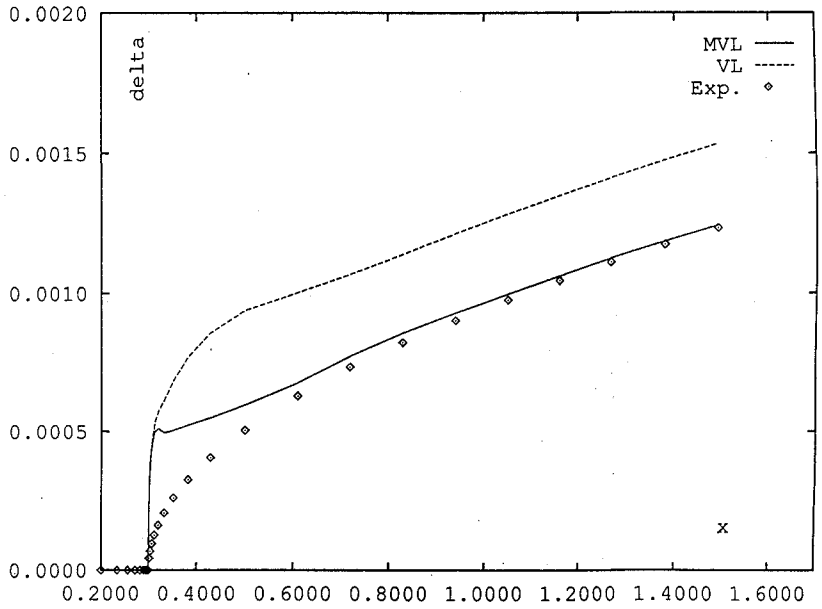

Fig. 1 Comparison of boundary-layer thickness δ vs x.

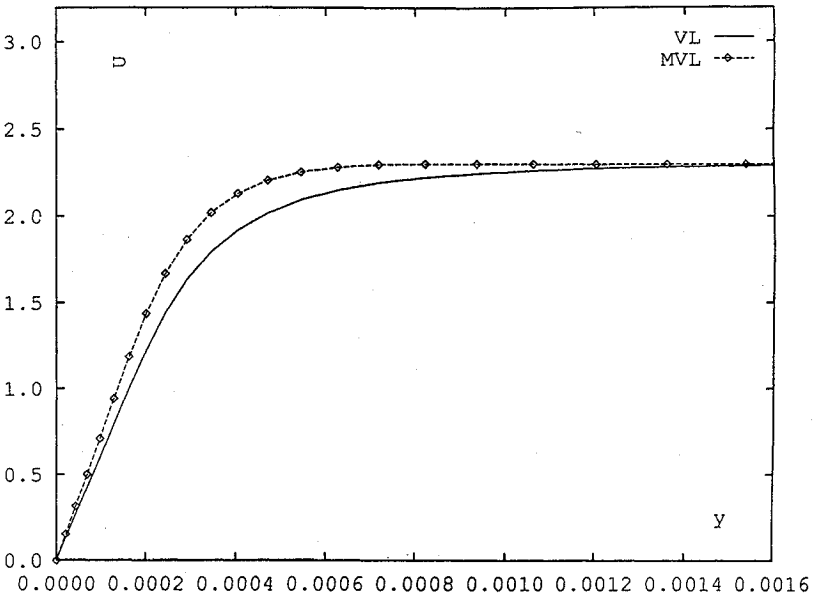

Fig. 2 Comparison of the VL and MVL method for velocity profile vs y for $x = 0.5$.

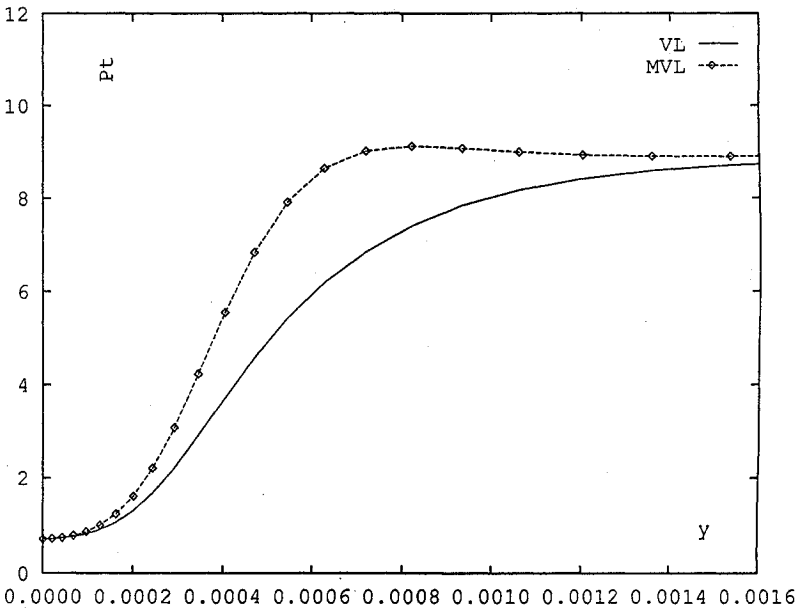

Fig. 3 Comparison of VL and MVL method for the total pressure profile vs y for $x = 0.5$.

When $M = M_l$:

$$\frac{\partial E^+_{\mathrm{MVL}}}{\partial M} = \frac{\partial E^+_{\mathrm{VL}}}{\partial M} \qquad \frac{\partial E^-_{\mathrm{MVL}}}{\partial M} = \frac{\partial E^-_{\mathrm{VL}}}{\partial M}$$

These conditions impose that for Ψ_{MVL} the following holds.
When $M = 0$:

$$\Psi_{\mathrm{MVL}} = 0 \qquad \frac{\partial \Psi_{\mathrm{MVL}}}{\partial M} = 0$$

When $M = M_l$:

$$\Psi_{\mathrm{MVL}} = 1 \qquad \frac{\partial \Psi_{\mathrm{MVL}}}{\partial M} = 0$$

Then, the monoticity condition is preserved.

It is possible to define a third-order polynomial, but a trigonometric function gives better results because the transition is smoother close to $M = 0$ and $M = M_l$.

If $|M| \leq M_l$,

$$\Psi_{\mathrm{MVL}} = \tfrac{1}{2}\{1 - \cos[\pi(M/M_l)]\}$$

If $|M| > M_l$,

$$\Psi_{\mathrm{MVL}} = 1$$

Thus, a single expression can be given for the entire domain:

$$\forall M \in]-\infty, +\infty[, \ \Psi_{\mathrm{MVL}} = \tfrac{1}{2}\{1 - \cos[\pi \max(1, |M/M_l|)]\}$$

This formulation is obtained without a specific local test but it still captures the shock well (only the VL flux is applied) and conserves high accuracy in the boundary layers (mainly CS flux is applied). Since the VL numerical viscosity is reduced or suppressed, a central numerical viscosity ΔE_{nv} must be added at fourth order, for example, and balanced by the function $(1 - \Psi_{\mathrm{MVL}})$ to ensure the stability with the following formulation:

$$\Delta E_{nv}(q_i) = (1 - \Psi_{\mathrm{MVL}})(\varepsilon_i/8)[q_{i+1} - 4q_{i+1} + 6q_i - 4q_{i-1} + q_{i-2}]$$

where ε_i is an adjustable coefficient. In fact, this viscosity is not always necessary because the numerical viscosity of the VL part can be sufficient. The value of ε_i is about 0.02.

For the three-dimensional case, the same formulation is applied in each direction for the three fluxes E, F, and G.

The choice of the linking Mach number is easy. To reduce the gradient of the weighting function, M_l must be equal to the highest possible value (but always less than 1); on the other hand, since the central scheme produces oscillations through shock, M_l must be less than the Mach number value just after the shock in transonic cases. We usually choose M_l equal to 0.6 in all directions for transonic applications.

Numerical Results

We present an example of comparative results on supersonic flow. The velocity is normalized by the upstream sound velocity $c_{-\infty}$, the density by the upstream density $\rho_{-\infty}$ and the pressure by $\rho_{-\infty}c^2_{-\infty}$.

We consider a supersonic laminar flow of air over a flat plate. The external flow, at Mach number 2.3 is prescribed by a static pressure p equal to 24,586 Pa and a density equal to 0.6 kg/m^3. The dynamic viscosity and the thermal diffusivity are constant. The flow is completely defined upstream. A no-slip boundary condition for the velocity and a fixed temperature of 270 K are imposed on the flat plate. The grid is made of 33 points in the streamwise x direction and 81 points in the spanwise y direction with a concentration of points near the leading edge (at $x = 0.3$) and near the plate (at $y = 0$) where the smallest cell height is 2.10^{-5} m.

Figure 1 compares the boundary-layer thickness δ between the semiempirical thickness law,[8] the VL method, and the MVL method. The boundary-layer thickness obtained by the VL method is large compare to the empirical one. This result confirms that at low Mach number the VL method is too diffusive. The boundary-layer thickness given by MVL method, however, is in very good agreement with the semiempirical law except near the leading edge. We can explain this difference by the weak oblique shock at the leading edge. The numerical integration that calculates δ detects the deficit of velocity through the shock and defines an excessive thickness of boundary layer even though it is a convective effect. The empirical law does not take this local effect into consideration. But the law is corrected to globally integrate the compressible effect, and this is why after $x = 0.6$, the thickness is the same as that found from the MVL method.

Comparison of the transverse profiles of velocity at $x = 0.5$ are given in Fig. 2 and show the important reduction of numerical viscosity in the boundary layer. The total pressure profile is drawn in Fig. 3 for $x = 0.5$. The horizontal slope for both methods is due to the heat transfer at the wall. In the boundary layer, the total pressure deficit is very important and this explains the deficit of velocity in the VL method. This explicitly illustrates the advantage of the MVL method for viscous flow.

Conclusion

A new MVL meathod has been developed that introduces a central scheme contribution in the low Mach number region. The expression of the VL flux is preserved and only conservative variable coefficients are modified in a MUSCL formulation. The results show conservation of robustness in shock capture and a dramatic improvement in the treatment of viscosity in the boundary layers.

References

[1]Van Leer, B., "Flux Vector Splitting for the Euler Equations," *Lecture Notes in Physics*, Vol. 170, 1982, pp. 501–512.

[2]Roe, P. L., and Baines, M. J., "Algorithm for Advection and Shock Problems," *Proceeding of the 4th Gamm. Conference on Numerical Methods in Fluid Mechanics*, edited by H. Viviand, Vieweg Verlag, Berlin, 1982.

[3]Liou, M. S., and Steffen, C. J., Jr., "High-Order Polynomial Expansions (HOPE) for Flux-Vector Splitting," NASA TM 104452, 1991.

[4]Ferrand, P., and Aubert, S., "Van Leer's Flux Splitting Extension at Low Mach Numbers," *Compte Rendu Académie des Sciences*, Paris, Vol. 317, Série II, 1993, pp. 1–4.

[5]Coirier, W. J., and Van Leer, B., "Numerical Flux Formula for the Euler and Navier–Stokes Equations: II. Progress in Flux Vector Splitting," AIAA Paper 91-1566, 1991.

[6]Coquel, F., and Liou, M.-S., "Field to Field Hybrid Up-Wind Splitting Methods," AIAA Paper 93-3302, 1993.

[7]Aubert, S., Hallo, L., Ferrand, P., and Buffat, M., "Numerical Behavior of Unsteady Waves," *AIAA Journal*, Vol. 33, No. 5, 1995, pp. 888–893.

[8]Cousteix, J., *Couche Limite Laminaire*, Cepadues Edition, 1988.

Efficient, Robust Second-Order Total Variation Diminishing Scheme

S.-M. Liang,* C.-J. Tsai,† and L.-N. Wu‡
National Cheng Kung University, Tainan, Taiwan 701, Republic of China

Introduction

HIGH-RESOLUTION schemes have been developed to capture discontinuities such as shock waves in the recent years.[1–3] One of the widely used schemes is the second-order total variation diminishing (TVD) scheme originally introduced by Harten.[2] The TVD scheme was obtained through the construction of flux limiters in numerical fluxes. There were several flux limiters suggested in the second-order TVD schemes.[4] Currently, there exists no rule for determining a better flux limiter among the existing limiters. A better flux limiter means one that makes the scheme used converge rapidly to a required tolerance for steady flow calculation and that can be used for a wide range of flows involving high-temperature effects. Numerical experience seems to be the only way. In this study, we report our past experiences on the use of implicit second-order TVD schemes associated with three flux limiters in calculations of the Euler equations for various compressible flow problems. Based on our test problems, an improved flux limiter was found for use with the implicit TVD scheme.

Contents

In this study, the implicit TVD scheme is constructed with three different flux limiters for solving the time-dependent Euler's equations. The first one is Harten's flux limiter

$$g_{j,k} = \text{minmod}\left(\alpha_{j-\frac{1}{2},k}, \alpha_{j+\frac{1}{2},k}\right) \tag{1}$$

where $\alpha_{j+(1/2),k} = (R_x^{-1})_{j+(1/2),k}(U_{j+1,k} - U_{j,k})$ are the characteristic variables evaluated at the interface $(j + \frac{1}{2}, k)$; R is the similarity transformation composed of the right eigenvectors of the Jacobian matrix; and the minmod function denotes the smallest number in absolute value in its arguments when the arguments are of the same sign and is equal to zero when the arguments are of opposite sign. The second one is the Yee flux limiter that is to replace the sum of $g_{j,k}$ and $g_{j+1,k}$ in the Harten scheme by minmod $(\alpha_{j-(1/2),k}, \alpha_{j+(1/2),k}, \alpha_{j+(3/2),k})$, i.e.,

$$g_{j,k} + g_{j+1,k} \leftarrow \text{minmod}\left(\alpha_{j-\frac{1}{2},k}, \alpha_{j+\frac{1}{2},k}, \alpha_{j+\frac{3}{2},k}\right) \tag{2}$$

In the past, we suggested another flux limiter that is slightly modified from Eq. (2) to drive the numerical residual to within a desired tolerance. The modification is to shift the index j one point upstream; namely, the suggested flux limiter is

$$g_{j,k} + g_{j+1,k} \leftarrow \text{minmod}\left(\alpha_{j-\frac{3}{2},k}, \alpha_{j-\frac{1}{2},k}, \alpha_{j+\frac{1}{2},k}\right) \tag{3}$$

With the improved flux limiter, the implicit TVD scheme is found to be more efficient than the scheme with Harten's or Yee's flux limiter. Note that the suggested flux limiter is implemented only in the implicit operator (the left-hand side) of the difference equation discretized from the Euler equations, since an implicit operator dictates the stability and the convergence rate of an implicit scheme. And the Harten flux limiter, Eq. (1), is used on the right-hand side of the difference equation to retain the spatial accuracy.

Received Feb. 25, 1995; revision received Aug. 21, 1995; accepted for publication Sept. 11, 1995.

*Professor, Institute of Aeronautics and Astronautics. Member AIAA.

†Graduate Student, Institute of Aeronautics and Astronautics; currently Associated Professor, National Tainan Teachers College, Tainan, Taiwan, ROC.

‡Graduate Student, Institute of Aeronautics and Astronautics.